Cancer Research

Using the Transcription Factor Inhibitor of DNA Binding 1 to Selectively Target Endothelial Progenitor Cells Offers Novel Strategies to Inhibit Tumor Angiogenesis and Growth

Albert S. Mellick[1], Prue N. Plummer[1], Daniel J. Nolan[2], Dingcheng Gao[2], Kathryn Bambino[2], Mary Hahn[2], Raul Catena[2], Vivian Turner[3], Kevin McDonnell[2], Robert Benezra[4], Robert Brink[3], Alexander Swarbrick[3], and Vivek Mittal[2]

Abstract

Tumor angiogenesis is essential for malignant growth and metastasis. Bone marrow (BM)–derived endothelial progenitor cells (EPC) contribute to angiogenesis-mediated tumor growth. EPC ablation can reduce tumor growth; however, the lack of a marker that can track EPCs from the BM to tumor neovasculature has impeded progress in understanding the molecular mechanisms underlying EPC biology. Here, we report the use of transgenic mouse and lentiviral models to monitor the BM-derived compartment of the tumor stroma; this approach exploits the selectivity of the transcription factor inhibitor of DNA binding 1 (Id1) for EPCs to track EPCs in the BM, blood, and tumor stroma, as well as mature EPCs. Acute ablation of BM-derived EPCs using Id1-directed delivery of a suicide gene reduced circulating EPCs and yielded significant defects in angiogenesis-mediated tumor growth. Additionally, use of the Id1 proximal promoter to express microRNA-30–based short hairpin RNA inhibited the expression of critical EPC-intrinsic factors, confirming that signaling through vascular endothelial growth factor receptor 2 is required for EPC-mediated tumor biology. By exploiting the selectivity of Id1 gene expression in EPCs, our results establish a strategy to track and target EPCs *in vivo*, clarifying the significant role that EPCs play in BM-mediated tumor angiogenesis. *Cancer Res; 70(18); 7273–82. ©2010 AACR.*

Introduction

The tumor microenvironment is composed mainly of bone marrow (BM)–derived cells, which are critical to angiogenesis-mediated tumor growth and spread (1). These include myeloid cells such as Tie-2$^+$ and GR-1$^+$ monocytes (2–5), tumor-associated macrophages (6, 7), inflammatory cells (8, 9), platelet-derived growth factor receptor β^+ pericytes (10), and endothelial progenitor cells (EPC; refs. 11–13). Of particular interest are the BM-derived EPCs, as they have been shown to play a significant role in the growth of early tumors and metastatic lesions by mediating the angiogenic switch (14–17). EPCs have also been proposed to provide an alternative source of tumor endothelium, and thus contribute to neovessel formation by directly incorporating into nascent vasculature as differentiated endothelial cells (11–13). Therefore, EPCs represent important new targets for novel antiangiogenic therapies without the side effects associated with current therapies, which also target host vasculature (14–17).

EPCs are detected as a unique cell population in the peripheral blood (PB), expressing a variety of cell surface markers, which identify them as vascular and BM-derived. Key EPC markers include vascular endothelial (VE)-cadherin, vascular endothelial growth factor receptor 2 (VEGFR2), CD31^{low}, c-kit, and prominin 1/AC133 (16–19). However, the expression of these markers differs depending on whether the EPCs are in the BM, PB, or tumor. This lack of a single marker to be able to unambiguously track EPCs has led to several recent cancer studies failing to identify EPCs in specific mouse tumor models (18–21). This has also raised concerns as to whether the same population is being truly monitored *in vivo*, and has imposed tremendous limitations on the assessment of the biological function of tumor-associated EPCs as well as their potential as targets for antiangiogenic cancer therapy.

Previous studies have shown that, like tumor-activated endothelium, BM-EPCs also express the transcription factor inhibitor of DNA binding 1 (Id1). Id1 is a member of the helix-loop-helix family of transcription factors and a marker

Authors' Affiliations: [1]School of Medical Science, Griffith University, Gold Coast, Queensland, Australia; [2]Weill Cornell University Medical College, New York, New York; [3]Garvan Institute of Medical Research, Sydney, Australia; and [4]Program in Cancer Biology and Genetics, Memorial Sloan-Kettering Cancer Center, New York, New York

Note: Supplementary data for this article are available at Cancer Research Online (http://cancerres.aacrjournals.org/).

Corresponding Authors: Albert S. Mellick, School of Medical Science, Griffith University, Parklands Drive, Gold Coast, QLD 4215, Australia. Phone: 61-7-55527273; Fax: 61-7-55528908; E-mail: a.mellick@griffith.edu.au or Vivek Mittal, Weill Cornell University Medical College, 525E 68th Street, 1300 York Avenue, New York, NY 10021. E-mail: vim2010@med.cornell.edu.

doi: 10.1158/0008-5472.CAN-10-1142

of self-renewal (22). We have previously shown that global inhibition of Id1 in the BM results in significant specific EPC-linked tumor vascular defects (17, 23). These findings nominate Id1 as a potential marker of EPCs.

The aims of this study were to determine if Id1 could be used to track EPCs *in vivo*, specifically target EPCs, and modify EPC-mediated tumor growth. Using a knock-in Id1 reporter mouse (24) and lentiviral (LV) transduction of BM transplanted (BMT) into wild-type (WT) recipients, we have shown that the Id1 gene activity can be used to track and modify BM-EPCs in the BM, blood, BM compartment of the tumor stroma, and luminally incorporated BM-EPCs. Furthermore, selective ablation of EPCs *in vivo*, using the Id1 proximal promoter (pr/p) to drive the expression of the suicide gene herpes simplex virus (*HSV*)-thymidine kinase (*tk*), resulted in specific EPC-linked vascular detects and impaired tumor growth. Directed delivery of short hairpin RNA inhibition (shRNAi) by the LV-Id1pr/p was also used to inhibit key EPC-linked factors, such as VEGFR2, resulting in marked EPC and angiogenesis-linked tumor growth defects. This work underscores the functional importance of EPCs in tumor biology and directly links EPC-intrinsic Id1 to EPC biology and EPC-mediated tumor vascular growth. It also shows that EPCs represent a unique lineage that can be tracked from the BM to tumor using Id1.

Materials and Methods

Mice

WT C57BL/6 mice, C57BL/6 $Id1^{+/GFP}$ transgenic reporter mice (24), and green fluorescent protein (GFP)–transgenic C57BL/6-Tg (ACTb-EGFP) 10sb/J mice expressing GFP under a hybrid chicken β-actin promoter and cytomegalovirus intermediate early enhancer (25) were purchased from The Jackson Laboratory. All procedures involving mice were conducted in accordance with protocols reviewed and approved by the institutional animal care and ethics committees.

Cell lines and growth conditions

Murine Lewis Lung Carcinoma cells (LLCs)/D122 (provided by Lea Eisenbach, Wiezmann Institute of Science, Rehovot, Israel), murine lymphoma cells B6RV2 (14), and murine endothelial cells (mHEVc; provided by J. Cook-Mills, University of Cincinnati, Cincinnati, OH; ref. 26) were maintained in RPMI with 15% fetal bovine serum. Murine myoblast progenitors C2Cl2 cells (American Type Culture Collection) and human kidney 293T cells were maintained in DMEM supplemented with 10% FCS.

Screening shRNAs

shRNAs targeting Id1 were cloned into a U6 or Id1 promoter–containing vector as described (27). shRNA targeting firefly luciferase served as a nonspecific control. SYBR Green I detection (28) was used for reverse transcription-PCR (RT-PCR) analysis using the ABI7700 real-time PCR detection system (Applied Biosystems). The primers used for RT-PCR analysis were *VEGFR2* (forward, 5′-ATCGTGTACATCACCGAGAACA-3′, and reverse, 5′-CGGCATAGCTGATCATGTAAC T-3′) and *Id1* (forward, 5′-GTACTTGGTCTGTCGGAGCAA-3′, and reverse, 5′-CATGTCGTAGAGCAGGACGTT-3′). For internal controls, *β-actin* (forward, 5′-TGTTTGAGACCTTCAACACC-3′, and reverse, 5′-TAGGAGCCAGAGCAGTAATC-3′) and *GAPDH* (forward, 5′-TCAACGACCCTTCATTGAC-3′, and reverse, 5′-ATGCAGGGATGATGTTCTGG-3′) were used.

Generation of LV constructs

To generate pWPT-Ω, a gateway destination cassette ccdB (Invitrogen) was inserted into the *Sal*I site in the LV pWPT (D. Torono, University of Geneva, Geneva, Switzerland), and shRNAs were transferred from shuttle vectors by gateway recombination. To generate Id1pr/p-GFP LV, a 1.32-kb fragment containing the murine proximal Id1 promoter was amplified from C57BL/6 mouse genomic DNA and inserted into the pWPT-LV, replacing the EF1α short promoter. To create Id1pr/p-red fluorescent protein (RFP), GFP was replaced (*Mlu*I/*Xho*I) with monomeric RFP (mCherry; ref. 29). To generate pWPT-Id1pr/p-GFPITK, the *HSV-tk* gene was amplified from pSHTK (provided by Ventura, Universidade de São Paulo, São Paulo, Brazil) and inserted downstream of GFP/RFP and an internal ribosome entry site (provided by Patrick Paddison, Cold Spring Harbor Laboratories, Cold Spring Harbor, NY). MicroRNA-30 (miR-30)–based shRNA was amplified from shuttle vectors and cloned downstream of GFP.

LV production, BM transduction, and transplantation

LV pseudotyped with the vesicular stomatitis virus G protein (VSVG) was generated by calcium phosphate transfection into 293T cells with three packaging constructs, pMDLg/pRRE, REV, and pVSVG, as described (30). Viral titer was determined by p24 ELISA (Perkin-Elmer) or fluorescence-activated cell sorting (FACS) analysis of LV-infected 293T cells in the presence of serum. LV transductions of lineage-depleted BM cells (multiplicity of infection of ~50) were performed in serum-free StemSpan SFEM medium (Stem Cell Technologies) in the presence of interleukin-3 (IL-3; 20 ng/mL), IL-6 (100 ng/mL), and stem cell factor (100 ng/mL) for 12 hours. For BMT, 5×10^5 lineage-depleted BM cells were injected into the tail veins of lethally irradiated (1,100 rad) C57BL/6 mice. After BMT, RT-PCR analysis was used to determine the transduction efficiency of LV-infected BM cells. DNA was isolated from the BM and subjected to RT-PCR using GFP-specific primers: forward, 5′-GCTCTGCCCTCTCATTGTACA-3′, and reverse, 5′-GTGAACAGCTCCTCGCCCTT-3′. A standard curve was generated from titrated target DNA, and the vector copy number was determined.

Analysis of tumors, blood, and BM by immunohistochemistry and microscopy

C57BL/6 mice were inoculated intradermally with 5×10^6 LLC or B6RV2 cells, and tumor size was monitored and analyzed by microscopy (16). For the analysis of circulating endothelial progenitors (CEP), tail blood was collected in anticoagulant buffer (PBS, 5 mmol/L EDTA); for the analysis of BM-EPCs, the BM was flushed from the bones. PB

mononuclear cells and BM mononuclear cells were isolated by gradient centrifugation using Histopaque 1077 (Sigma) and then either cytospun onto Superfrost slides or stained for FACS analysis. Primary antibodies, CD31/platelet/endothelial cell adhesion molecule 1 (clone MEC 13.3), VE-cadherin/CD144 (clone 11D4.1), CD11b (clone M1/70), VEGFR2/Flk1 (clone avas12α1), GR-1 (clone RB6-8C5), pan CD45 (clone 30-F11), B220 (clone RA3-6B2), CD3 (clone 500A2), c-kit/CD117 (clone 2B8), TIE2 (clone 33), and TER-119 (clone TER-119), were obtained from BD Pharmingen; prominin 1 (clone 13A4) was from eBiosciences; and Ki-67 (clone SP6) was from NeoMarkers. Unless otherwise stated, EPCs/CEPs were selected as VE-cadherin$^+$, VEGFR2$^+$, c-kit$^+$, CD45$^-$, and CD11b$^-$ subpopulations isolated by FACS from the mononuclear population in the BM/blood. Myeloid populations were selected as CD11b$^+$ (myeloid cells) and GR-1$^+$ (neutrophils), Tie-2$^+$ (Tie-2$^+$ monocytes), B220$^+$ (B cells), or CD3$^+$ (T cells), and isolated by FACS from the mononuclear population in the blood or BM. All populations were negative for TER119 (erythroid marker).

Microscopy was performed using 30-μm-thick sections, stained with Alexa Fluor–conjugated primary antibodies

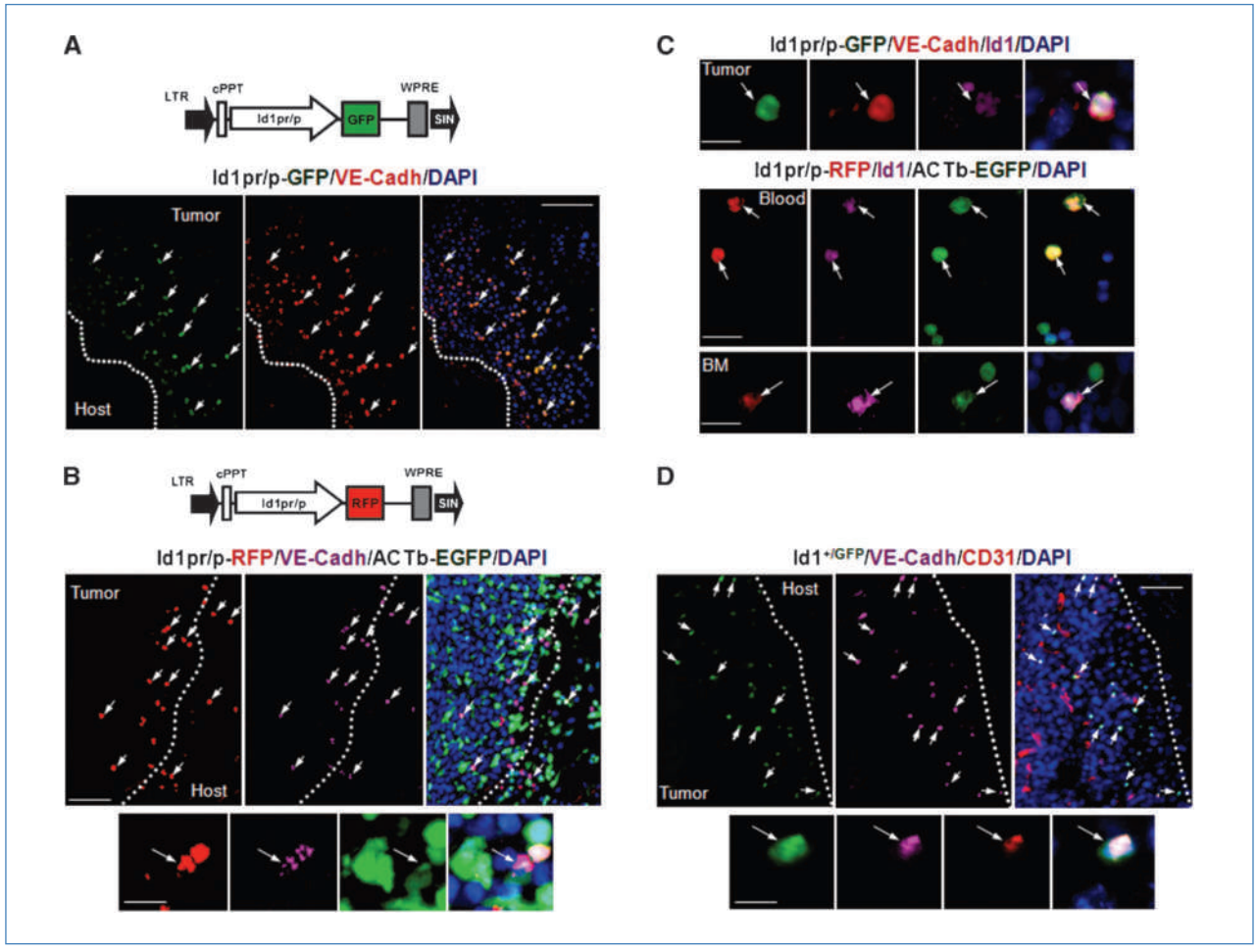

Figure 1. Id1 marks EPCs in the PB, BM, and tumor stroma. A, top, schematic of Id1pr/p-GFP LV vector: Id1pr/p driving GFP expression. cPPT, central polypurine tract; WPRE, woodchuck hepatitis virus post transcription regulatory element; LTR, long terminal repeat; SIN, self-inactivating. Bottom, microscopic images showing the recruitment of Id1pr/p-GFP$^+$ cells to the periphery of early nonvascularized LLC tumors (arrows; day 8, n = 15) in Id1pr/p-GFP BMT mice. Bar, 50 μm. B, top, schematic of Id1pr/p-RFP LV vector: Id1pr/p driving monomeric RFP/mCherry expression. Bottom, microscopic images showing the recruitment of Id1pr/p-RFP$^+$ cells to the periphery early nonvascularized LLC tumors (arrows; day 8, n = 15) in Id1pr/p-RFP/ACTb-EGFP BMT mice. Bar, 50 μm. High-resolution (×63) images show that Id1pr/p-RFP$^+$ cells can be used to mark and distinguish BM-derived ACTb-EGFP$^+$ VE-cadherin$^+$ BM-EPCs (arrow) from the other BM cells in the tumor stroma. Bar, 10 μm. C, top, image showing that the LV-Id1pr/p-GFP construct can be used to mark Id1 protein expressing VE-cadherin$^+$ BM-EPCs (arrow) in the tumor stroma. Bar, 10 μm. Bottom, high-resolution (×63) microscopic images of cytospun BM and PB from LLC tumor–challenged ACTb-EGFP/Id1pr/p-RFP BMT animals, showing that Id1pr/p$^+$ EPCs in the BM and PB express nuclear Id1 protein (white arrows). Bar, 20 μm. D, top, microscopic images showing vasculature and BM-derived Id1$^{+/GFP+}$ VE-cadherin$^+$ CD31^{low} BM-EPCs as part of the tumor stroma (arrows) of LLC tumors (day 15) implanted into Id1$^{+/GFP+}$ BMT mice (n = 10). Bar, 50 μm. Bottom, high-resolution (×63) images of BM-derived Id1$^{+/GFP+}$ VE-cadherin$^+$ CD31^{low} BM-EPCs (arrow) in the tumor stroma of LLC tumors (day 15) implanted into Id1$^{+/GFP+}$ BMT mice. Bar, 10 μm.

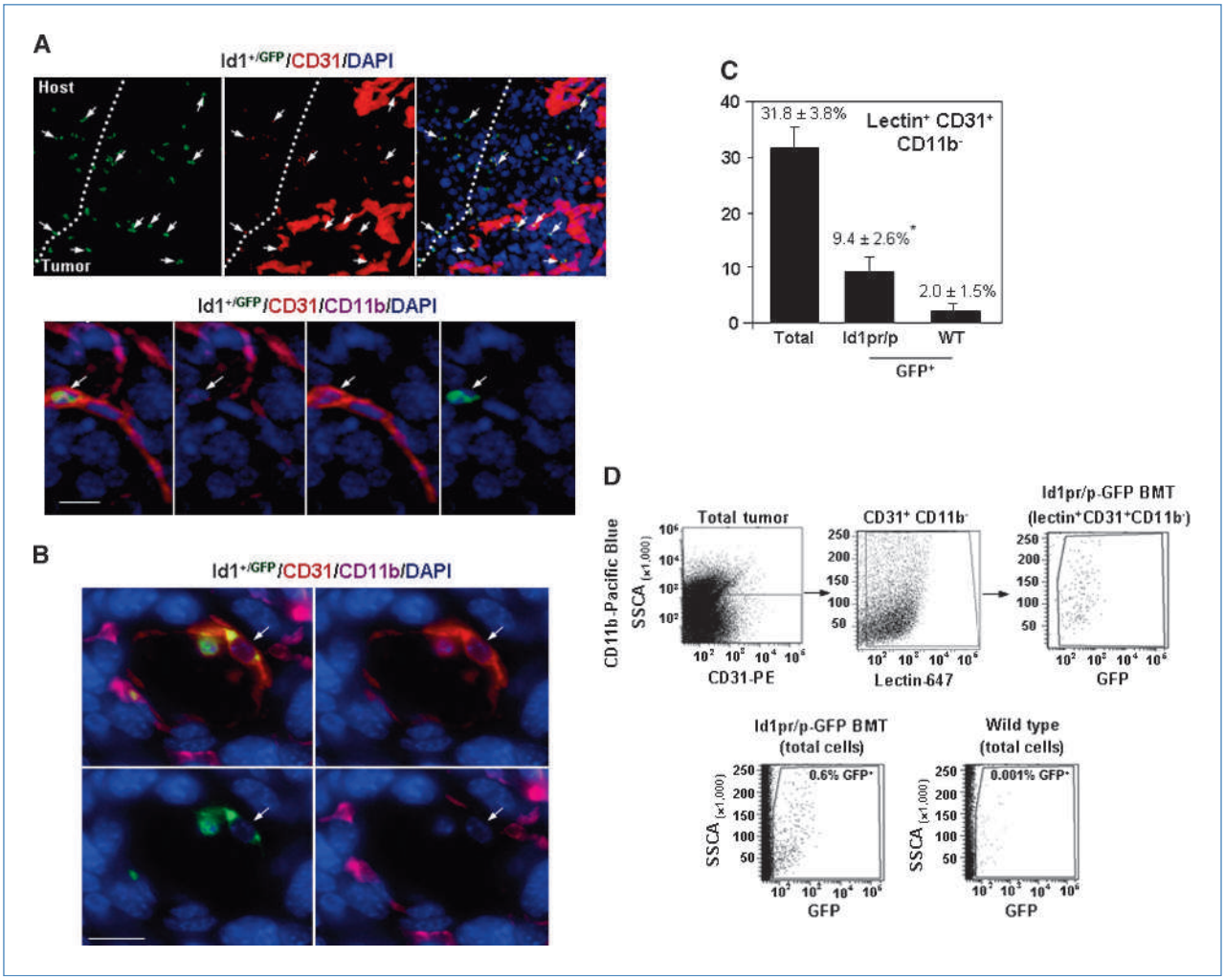

Figure 2. Id1 marks luminally incorporated, mature EPCs in the nascent tumor vasculature. A, top, microscopic images showing vasculature and BM-derived Id1$^{+/GFP+}$ CD31^{low} CD11b^{-} BM-EPCs as part of the tumor stroma (arrows) of LLC tumors (day 15) implanted into Id1$^{+/GFP+}$ BMT mice (n = 10). Bar, 50 μm. Bottom, microscopic images of a tumor vessel showing an incorporated BM-derived mature EPC (Id1$^{+/GFP+}$ CD31^{+} CD11b^{-}; arrow) in LLC tumors (day 15) implanted into Id1$^{+/GFP+}$ BMT mice. Bar, 20 μm. B, high-resolution (×63) transverse immunofluorescent images of a tumor vessel showing an incorporated BM-derived mature EPC (Id1$^{+/GFP+}$ CD31^{+} CD11b; arrow) in LLC tumors (day 15) implanted into Id1$^{+/GFP+}$ BMT mice. Bar, 20 μm. C, summary of FACS analysis showing the contribution of Id1^{+} mature EPCs in functional vessels by isolectin staining in LLC tumor (day 6) in Id1pr/p-GFP BMT mice. D, representative scatter plots showing derivation of GFP gates. SSCA, side scatter values.

with 4′,6-diamidino-2-phenylindole staining for cell nucleus (Invitrogen). In some cases, Alexa Fluor–conjugated secondary antirabbit antibodies were used for staining with anti-Id1 monoclonal antibody (22). RFP/GFP^{+} cells were detected by their own signal. Fluorescent images were obtained using a Zeiss fluorescent microscope (Software Axiovision LE 4) with resolutions of 0.275 to 0.35 μm as described (16).

FACS analysis

Single-cell suspensions were preblocked with F_c block (CD16/CD32, BD Pharmingen) and incubated with primary antibodies; these include IgG2aκ and IgG2aβ isotype controls and various antibodies described previously. Labeled cells were measured by a LSRII flow cytometer (Becton Dickinson), and compensation was measured by FACSDiva software (BD Immunocytometry Systems). Animals were also injected with Alexa Fluor 647–conjugated isolectin GS-IB$_4$ (50 μg for 10 minutes; Molecular Probes) before sacrifice. Multivariate FACS was performed using isotype antibodies, fluorescence-minus-one samples, and unstained samples for determining appropriate gates, voltages, and compensation (31).

Statistics and data analysis

Statistical analysis was performed using GraphPad Prism software (version 3.0). Statistical analysis of tumor growth by one-way ANOVA (α = 0.05) was used to compare different treatments. For comparison of groups at end point, Student's t test (α = 0.05) was used. Unless otherwise stated, data are presented as mean ± SEM.

Results

Id1 is upregulated in the BM and tumor-associated EPCs

Gene expression profiling showed that Id1 was one of several genes significantly upregulated at least 4-fold in BM stem cells obtained from tumor-challenged mice (Supplementary Fig. S1A). As Id1-knockout mice exhibit impaired EPC-linked angiogenic and tumor growth defects (14, 19), we next determined to localize Id1 to specific BM-derived cell populations in the tumor stroma. To do this, we transplanted the BM from β-actin (ACTb)-EGFP mice (25) into irradiated age-matched, syngeneic, WT recipients and examined preangiogenic, as well as vascularized, tumors after intradermal inoculation of LLC cells. Notably, Id1 protein was confined to BM-derived GFP$^+$ VE-cadherin$^+$ EPCs (16) and not to other BM-derived GFP$^+$ myeloid cells (Supplementary Fig. S1B).

The Id1 gene activity marks EPCs in the BM, blood, and tumor stroma

To determine whether a genetic strategy using the Id1 gene activity might be used to track EPCs and investigate EPC function *in vivo*, the pr/p of Id1 (1.32 kb), containing

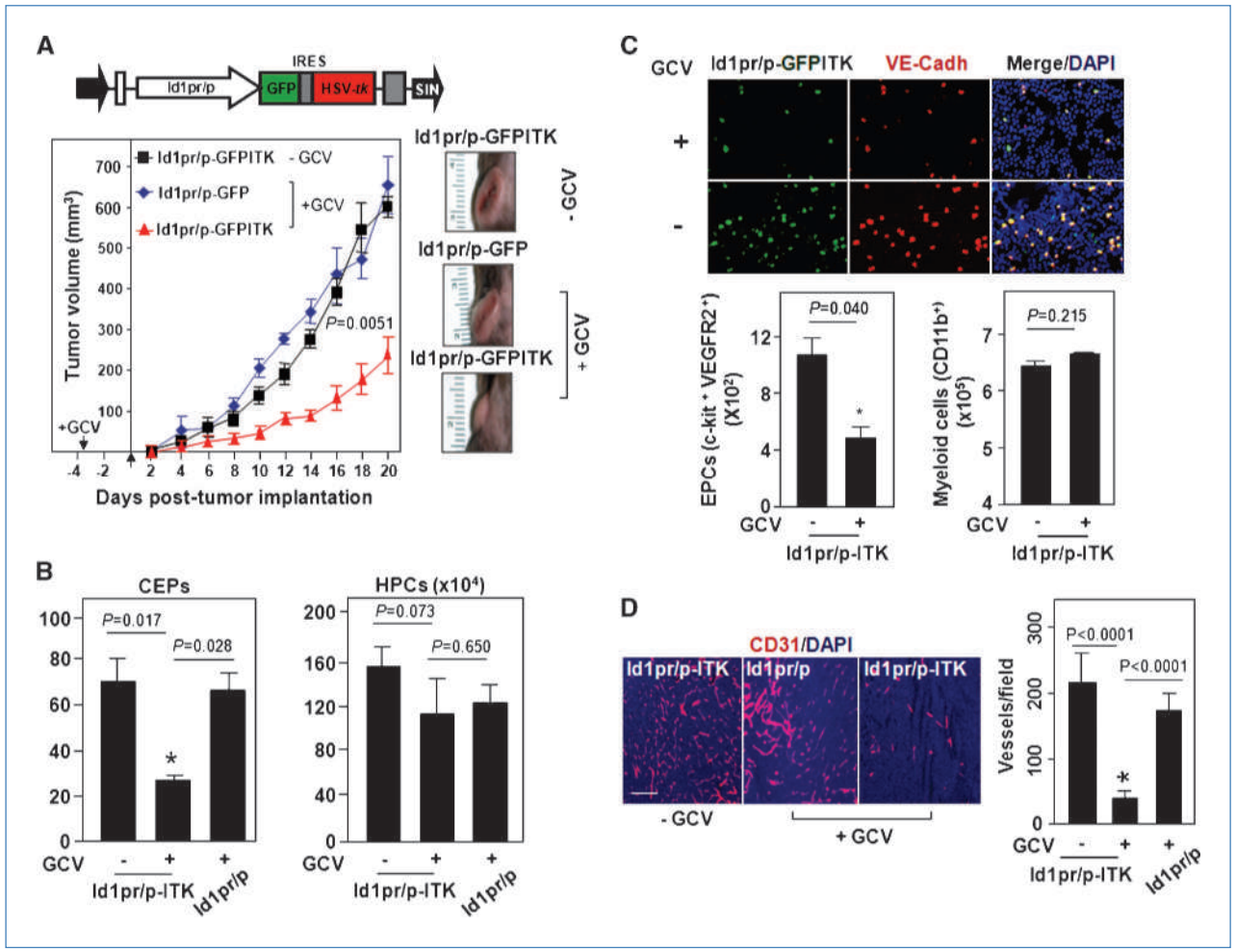

Figure 3. Selective elimination of Id1pr/p$^+$ EPCs by delivery of the suicide gene *HSV-tk* impairs tumor growth. A, top, schematic of Id1pr/p LV vector with Id1pr/p driving GFP and *HSV-tk* expression. Bottom, LLC tumor growth (mean ± SEM) and morphology in Id1pr/p-GFPITK BMT mice (n = 10) and Id1pr/p-GFP BMT mice (n = 5), either treated with GCV (+GCV) or untreated (–GCV). Similar trends were observed in a repeat experiment. B, FACS analysis of PB from tumor-challenged Id1pr/p-GFPITK (+GCV), Id1pr/p-GFPITK (-GCV), and GCV control Id1pr/p-GFP (+GCV) BMT mice, showing the number of mobilized CEPs (c-kit$^+$ VEGFR2$^+$) and HPCs (c-kit$^+$ CD45$^+$). A total of 1 × 10^6 cells were analyzed per animal. Data are represented as mean number of cells per 1 × 10^5 PB mononuclear cells ± SEM (n = 5 per group); analyzed by Student's t test. C, top, microscopic analysis of EPCs (VE-cadherin$^+$ GFP$^+$) from the BM after GCV treatment in Id1pr/p-GFPITK BMT mice. Bottom, FACS analysis of the BM from tumor-challenged Id1pr/p-GFPITK (–GCV or +GCV) BMT mice, showing the number of EPCs (c-kit$^+$ VEGFR2$^+$) and myeloid cells (CD11b$^+$). Data show significant difference between GCV-treated Id1pr/p-GFPITK and untreated animals (P = 0.040, by Student's t test). Numbers are normalized per 1 × 10^6 BM mononuclear cells. D, CD31$^+$ immunostaining showing a lower vessel density in Id1pr/p-GFPITK +GCV LLC tumors compared with Id1pr/p-GFPITK –GCV and Id1pr/p LLC tumors (n = 15). Bar, 100 μm. Data are represented as average number of vessels per field ± SEM (analyzed by Student's t test).

known Id1 regulatory sequences (32) and driving fluorescent reporter genes (GFP and RFP/mCherry), were cloned into the pWPT, a self-inactivating LV vector (ref. 29; Fig. 1A and B, top). The functionality of the Id1pr/p constructs was confirmed after stable transduction. In this experiment, dose-dependent enhancement of reporter activity was observed after administration of serum (not shown) or growth factors to cell lines stably transduced with the LV-Id1pr/p constructs (Supplementary Fig. S2A).

To evaluate the selectivity of Id1pr/p for EPCs *in vivo*, BM cells not yet expressing key lineage markers (lineage-depleted BM; see Materials and Methods), obtained from WT mice, were transduced with Id1pr/p-GFP *ex vivo* and transplanted into irradiated WT recipients. To determine the relative abundance of EPCs with respect to other BM-derived cells, lineage-depleted BM cells derived from ACTb-EGFP$^+$ mice were also transduced with LV-Id1pr/p-RFP. After BM engraftment, RT-PCR analysis showed an average of two to four LV integrations per cell (Supplementary Fig. S2B). Id1pr/p-GFP/WT and Id1pr/p-RFP/ACTb-EGFP$^+$ BMT animals were then LLC tumor challenged. Analysis of early tumors (days 6–8) showed recruitment of Id1pr/p-GFP/RFP$^+$ VE-cadherin$^+$ cells to the tumor periphery (Fig. 1A and B, bottom). In addition to VE-cadherin, these cells also expressed other EPC markers (16), including VEGFR2 and prominin 1 (Supplementary Fig. S3A and B). Furthermore, none of these Id1pr/p$^+$ cells expressed the myeloid marker CD11b, thus indicating that these cells are EPCs (Supplementary Fig. S3C). In the blood, reporter analysis showed that the majority of VEGFR2$^+$ c-kit$^+$ CD11b$^-$ CEPs (80%; $P < 0.001$) were Id1pr/p$^+$, whereas BM hematopoietic cells of the myeloid lineage expressed negligible levels of Id1pr/p activity (0.09%; $P < 0.001$; Supplementary Fig. S4A and B; Supplementary Table S1). Additionally, analysis of the BM showed that Id1pr/p activity was restricted to VE-cadherin$^+$ CD11b$^-$ cells (66.83%; $P < 0.001$), thus indicating that the Id1pr/p are marking EPCs (Supplementary Fig. S4C; Supplementary Table S1). Finally, the Id1pr/p$^+$ cells also expressed endogenous Id1 protein in the blood, BM, and tumor stroma (Fig. 1C).

To confirm that we had captured the important regulatory regions in the LV constructs used and to determine whether the observed effects were due to positional effects or chromosomal positioning of the LV vector, we took advantage of the recently available Id1$^{+/GFP}$ knock-in fluorescent reporter mice (24). In this experiment, the BM from these mice was transplanted into irradiated WT mice, and tissues were examined in the context of LLC tumor challenge. In confirmation of the LV work, GFP activity was exclusively restricted to VE-cadherin$^+$ CD31^{low} CD11b$^-$ BM-derived cells (EPCs) in the tumor stroma of early tumors [Figs. 1D and 2A (top)].

The Id1 gene activity marks mature EPCs incorporated as part of the functional tumor vasculature

Analysis of later tumors (days 8–12) from LV and Id1$^{+/GFP}$ BMT mice revealed luminally incorporated GFP$^+$ CD31$^+$ CD11b$^-$ mature EPCs in a subset of tumor neovessels [Fig. 2A (bottom) and B; Supplementary Fig. S5A and B]. This shows that the Id1pr/p also marks mature EPCs incorporated as endothelial cells (16). We next quantified these luminally incorporated BM-derived Id1$^+$ endothelial cells by FACS after administration of isolectin GS-IB4 (16). Of the total functional vasculature, as determined by lectin$^+$ CD31$^+$ CD11b$^-$ cells, 9.4 ± 2.6% of the vessel-incorporated luminal endothelial cells (GFP$^+$ lectin$^+$ CD31$^+$ CD11b$^-$) at day 8 were BM-derived and expressed the Id1pr/p (Fig. 2C and D).

Ablation of Id1$^+$ cells results in angiogenesis inhibition and impaired tumor growth

To determine the biological function of EPCs in tumor angiogenesis and to accomplish selective EPC ablation, the Id1pr/p-LV was used to express the suicide gene *HSV-tk* (ref. 33; Fig. 3A, top; Supplementary Fig. S6A–C). This was done by transducing lineage-depleted BM cells with the LV-Id1pr/p-GFPITK and transplanting these cells into irradiated WT recipients. The administration of ganciclovir (GCV) showed a significant delay in tumor growth in Id1pr/p-GFPITK mice (~70%, by day 20) compared with controls (Fig. 3A, bottom).

FACS analysis showed that GCV treatment resulted in an ~3-fold reduction in CEPs in the PB of Id1pr/p-GFPITK mice (Fig. 3B). As there was no significant change in other BM-derived hematopoietic cells or progenitors, it can be concluded that this reduction was CEP specific (Fig. 3B). We next sought to determine whether this reduction in CEPs was due to *tk*-mediated BM-EPC ablation. Analysis of the BM showed a >2-fold reduction in EPCs, with no significant reduction in CD11b$^+$ hematopoietic cells in Id1pr/p-GFPITK (+GCV) mice (Fig. 3C). In concordance with this observation, actively proliferating EPCs were observed in tumor-challenged BM, as judged by Ki-67 staining (ref. 34; Supplementary Fig. S6D). The Id1pr/p-GFPITK (+GCV) tumors also showed a significant reduction in vessel density and growth compared with untreated Id1pr/p-GFPITK controls (Fig. 3D; $P < 0.0001$). These results show that Id1pr/p-mediated delivery of *tk*, while resulting in the selective elimination of EPCs, seemed to also be associated with limited bystander effects, a complicating factor in many GCV/*tk*–based approaches (35).

Id1-directed silencing of EPC-intrinsic factors results in inhibition of angiogenesis-mediated tumor growth

To determine whether EPC-intrinsic factors, such as Id1 and VEGFR2, were required for EPC-mediated tumor angiogenesis and whether Id1 ablation specifically affected EPC biology in the context of tumor challenge, we used short hairpin (Ω) RNAi, delivered by the LV-Id1pr/p construct, to directly inhibit BM-EPCs. First, to assess LV-mediated shRNA delivery *in vivo*, vectors with the constitutive U6 promoter driving RNAi were used (Supplementary Fig. S7A and B, top). As expected from the EPC-linked tumor angiogenesis defects observed in Id1-knockout mice (14), BM-wide suppression of Id1 resulted in impaired B6RV2 lymphoma (Supplementary Fig. S7B, bottom right) and LLC (Supplementary Fig. S7B, bottom left) tumor growth. This finding was associated with reduced tumor vascularization and Id1 mRNA suppression (Supplementary Fig. S7C and D).

To facilitate expression by the polII Id1 promoter, miR-30–based shRNAs (36) were then cloned into LV-Id1pr/p (Fig. 4A,

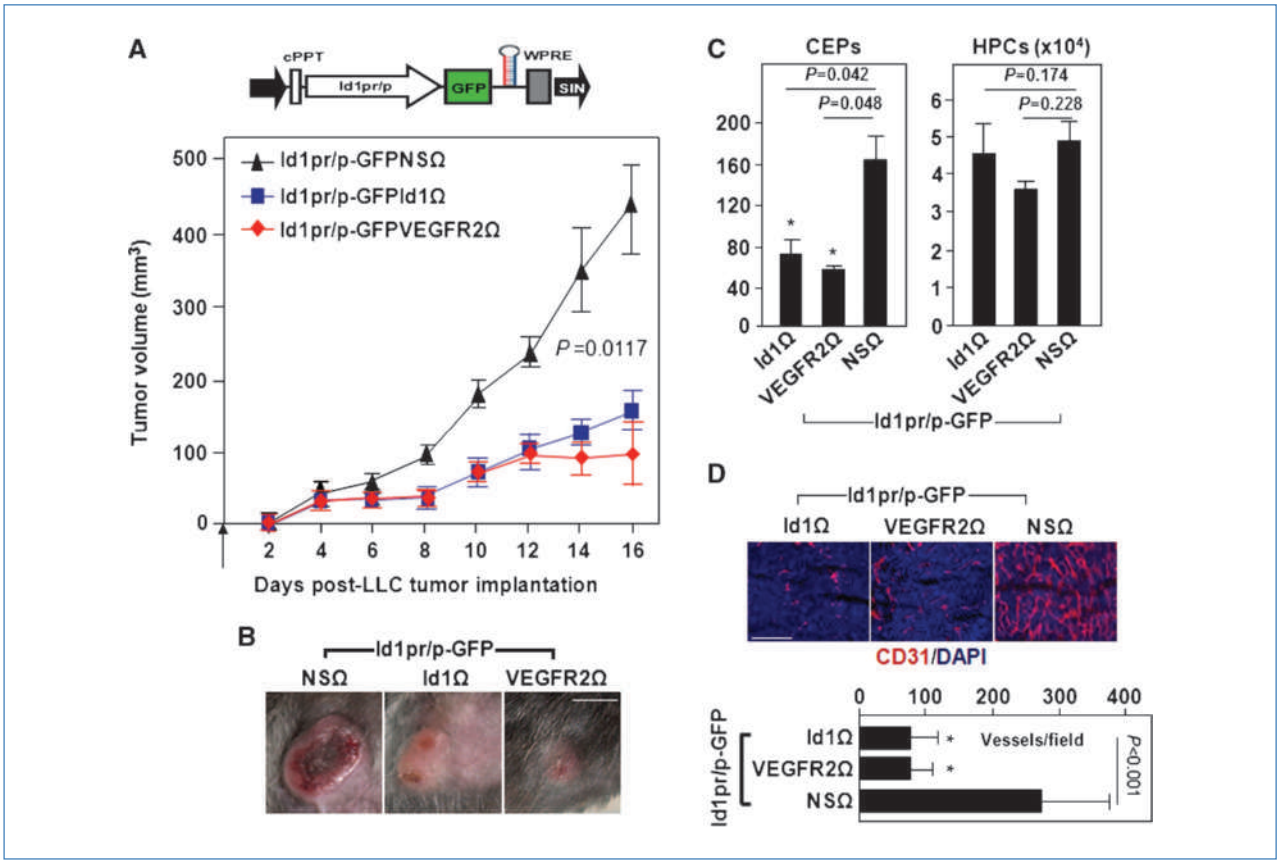

Figure 4. Id1pr/p shRNA–mediated suppression of VEGFR2 and Id1 in the EPCs results in angiogenesis inhibition and impaired tumor growth. A, top, schematic of Id1pr/p-GFPΩ LV vector with Id1 promoter driving GFP and miR30-based Ω expression. Bottom, LLC tumor growth in Id1pr/p-GFPNSΩ, Id1pr/p-GFPId1Ω, and Id1pr/p-GFPVEGFR2Ω BMT mice. Data are represented as mean volume ± SEM (n = 5 per group; P = 0.0117 by Student's t test). B, LLC tumor morphology in Id1pr/p-GFPNSΩ, Id1pr/p-GFPId1Ω, and Id1pr/p-GFPVEGFR2Ω BMT mice. Bar, 5 mm. C, FACS analysis of PB showing the number of CEPs (c-kit$^+$ VEGFR2$^+$) and HPCs (c-kit$^+$CD45$^+$) from LLC tumor–challenged Id1pr/p-GFPΩ mice. Data are represented as mean number of cells per 1 × 10^5 ± SEM (n = 5 per group; P values by Student's t test). This experiment was repeated and similar trends were observed. D, CD31$^+$ immunostaining showing a higher vessel density in Id1pr/p-GFPNSΩ LLC tumors compared with Id1pr/p-GFPId1Ω and Id1pr/p-GFPVEGFR2Ω LLC tumors (n = 15). Bar, 100 μm. Data are represented as average number of vessels per field ± SEM (analyzed by Student's t test).

top). The effectiveness of the LV-Id1pr/p constructs to drive each shRNAi, after stable integration, was determined using fluorescence and quantitative RT-PCR (Supplementary Fig. S8A and B). Next, WT lineage-depleted BM was transduced with Id1pr/p-GFPNSΩ, Id1pr/p-GFPId1Ω, and Id1pr/p-GFPVEGFR2Ω LV constructs, respectively, and transplanted into irradiated WT mice. Tumor growth in Id1pr/p-GFP Id1Ω and VEGFR2Ω BMT animals was impaired compared with nonspecific control [Fig. 4A (bottom) and B]. Notably, Id1pr/p shRNA–mediated suppression of both Id1 and VEGFR2 resulted in a 2- to 3-fold reduction of CEPs (Fig. 4C; Supplementary Fig. S9A), but no significant change in CD45$^+$/c-kit$^+$CD45$^+$ hematopoietic cells (Fig. 4C; Supplementary Fig. S9B and C), GR-1$^+$ neutrophils (Supplementary Fig. S9D), Tie2$^+$ monocytes, B220$^+$ B cells, CD3$^+$ T cells, or CD11b$^+$ c-kit$^+$ myeloid progenitors (Supplementary Fig. S10A–D), thus indicating that the effect of this suppression is CEP specific.

Analysis of tumors also showed a significant reduction in vessel density in Id1pr/p-GFPId1Ω and Id1pr/p-GFPVEGFR2Ω BMT mice compared with control mice (Fig. 4D). RT-PCR analysis of the BM confirmed that Id1 or VEGFR2 shRNAs had indeed suppressed cognate target genes *in vivo*. A 60% reduction in Id1 mRNA was observed in Id1Ω BM, whereas a 75% reduction was observed in VEGFR2 mRNA in VEGFR2Ω BM compared with NSΩ BM. The levels of pan hematopoietic CD45 mRNA also remained unchanged (Supplementary Fig. S8C). This experiment was not influenced by differential LV transduction efficiency or shRNA-mediated preferential enrichment of specific populations, as the BM of all Id1pr/p-GFPΩ–transduced animals showed comparable integrations per cell (Supplementary Fig. S8D). Taken together, these results show that the EPC-intrinsic expression of Id1 and VEGFR2 is critical for effective EPC mobilization from the BM and for normal tumor vascularization and growth.

Discussion

Whereas the contribution of BM-derived EPCs to tumor neovessel formation has been reported in mice and humans (12, 16, 37, 38), the inability to deliver transgenes specifically

to EPCs *in vivo* has precluded the analysis of their biological function and the assessment of their therapeutic potential. In this study, we show for the first time, using LV Id1 reporter constructs and $Id1^{+/GFP}$ fluorescent reporter mice (24), that the Id1 gene is selective for EPCs and can be used to track EPCs in the BM, blood, and tumor stroma and EPCs incorporated in the tumor vasculature. This identification of luminally incorporated mature EPCs in the tumor vasculature expressing the Id1 gene also validates that Id1 marks cells that are true EPCs. Furthermore, this finding validates that EPCs incorporate into the tumor vasculature. To the best of our knowledge, this study provides the first direct *in vivo* evidence of EPCs being marked by a single unique marker in each of these tissues.

To confirm the selectivity of Id1 for BM-EPCs, the LV-Id1pr/p construct was used to deliver the suicide transgene *HSV-tk*. After administration of GCV, EPCs were specifically ablated, resulting in a 60% to 70% reduction in CEPs, as well as angiogenesis inhibition and impaired tumor growth. This Id1-directed specific EPC ablation also did not significantly affect hematopoiesis or other hematopoietic cell populations. These findings are consistent with the observations in Id1-knockout mice and their WT littermates, which showed no difference in hematopoietic progenitors (HPC; ref. 39). Furthermore, although recent studies have shown that continuous serial transplantation of Id1-knockout BM results (ultimately) in impaired engraftment potential [due to a reduction in long-term repopulating hematopoietic stem cells (HSC)], Id1 was found to be dispensable for the short-term recovery of HSCs (24, 40). This is supported by the observation in this study that acute suppression of Id1 in the adult BM compartment, although resulting in tumor angiogenic defects, was not associated with HSC defects in our *HSV-tk*/GCV–treated animals.

The LV-Id1pr/p construct was also designed to express shRNAi designed after an endogenous miRNA and determine the function of the endogenous EPC-specific genes *Id1* and *VEGFR2* in tumor angiogenesis. shRNA-mediated suppression of Id1 resulted in EPC mobilization defects (a 70–80% reduction in CEPs) associated with severe angiogenesis inhibition and impaired tumor growth, with no significant change in cells of the hematopoietic lineage (B cells, T cells, $CD11b^+$ myeloid cells, and $Tie2^+$ monocytes). This result is consistent with the observations made following the *HSV-tk* delivery in Id1 transgenic mice (14, 24). However, our result differs slightly from that of Jankovic and colleagues (40), who reported reduced number of circulating lymphocytes in the PB of resting Id1-knockout mice. Possibly, in our study, acute and short-term suppression of Id1 in the BM compartment is devoid of the developmental compensations in the hematopoietic system associated with the Id1-knockout animal. In another study, Lyden and colleagues (14) showed that angiogenesis inhibition in the Id1 mutant was due to defects in mobilization of both $VEGFR2^+$ EPCs and $VEGFR1^+$ $CD11b^+$ hematopoietic cells. However, the use of the combined $Id1^{+/-}Id3^{null}$ genotype in their study may have resulted in defects in $VEGFR1^+$ cell mobilization as a result of Id3 loss, as described (41). Furthermore, we have observed that Id1 silencing (either by shRNAi or in Id1-knockout mice) specifically affects $VEGFR2^+$ EPCs and not $VEGFR1^+$ cells (20). Gao and colleagues (17) showed that suppression of Id1 in the whole BM by shRNAi leads to EPC and tumor angiogenic defects. In this study, restricted delivery of shRNAi to $Id1^+$-expressing cells using the Id1 promoter provides further compelling and direct evidence for the role of Id1 in EPC mobilization in the context of tumor challenge.

Similarly, EPC-specific VEGFR2 knockdown also resulted in loss of EPC function associated with vessel loss and impaired tumor growth. Notably, administration of VEGFR2 blocking antibody has been previously shown to have antiangiogenic effects (19); however, anti-VEGFR2 antibody is not specific to EPCs and also recognizes VEGFR2 expressed on endothelial cells in nascent blood vessels (42). Therefore, it has been difficult to discern whether the antiangiogenic phenotype observed in these studies is due to targeting EPCs, mature vessels, or both. Given that VEGFR2 suppression was strictly confined to the EPCs in the BM microenvironment, our results provide the most direct evidence for the role of VEGFR2 in EPC-mediated tumor angiogenesis.

Although luminally incorporated BM-derived $Id1pr/p^+$ endothelial cells represent a small fraction of the total tumor vasculature, specific ablation showed that EPCs play a critical role in angiogenesis-mediated tumor growth. We have previously shown that tumor-recruited EPCs secrete proangiogenic factors (20), suggesting that, in addition to providing structural support to nascent vessels, EPCs have paracrine function in vessel recruitment. This makes them uniquely important targets for antiangiogenic cancer therapy. However, our results do not discount the perivascular role of other tumor-recruited BM-derived hematopoietic cells (2, 7). Conceivably, each component of the tumor stroma plays a distinct role in tumor progression, and elimination of specific cell populations may drastically affect tumor growth. Furthermore, variability in reported contribution of EPCs across different mouse tumor models or strains [0%, Purhonen and colleagues (21); 2–20%, Nolan and colleagues (16); to 90%, Lyden and colleagues (14); summarized in a review by Gao and colleagues (43)] means that there is a need for a method to dynamically track and stage EPC involvement. Therefore, given that the role of tumor-associated BM-EPCs in cancer progression remains a subject of debate, the selectivity of Id1 for EPCs and its study through gene manipulation *in vivo* provide a key tool for further investigation. Furthermore, as the BM contributes to the tumor microenvironment, LV delivery of tissue-specific promoters driving RNAi may be used to understand the role of BM-derived cells in tumor biology.

Disclosure of Potential Conflicts of Interest

No potential conflicts of interest were disclosed.

Acknowledgments

We thank Yuri Lazebnick (CSHL) for comments on the manuscript; Margaret Black (Washington State University) for technical advice on *HSV-tk* experiments; and Raul Cantena (Weill Cornell Medical College), Pamela Moody, Anne Marie Torres (Flow Cytometry Facility, CSHL), Chris Brownlee

(Flow Facility, Garvan Institute), Lisa Bianco, Jodi Cobentz, Lea Manzella (Animal Facility, CSHL), and Diane Muller (Zeiss, Australia) for experimental and technical assistance.

Grant Support

NIH (http://www.nih.gov; V. Mittal), the Neuberger Berman Lung Cancer Laboratory (V. Mittal), the Robert I. Goldman Foundation (V. Mittal), the Australian Research Council (http://www.arc.gov.au; A. Mellick), the Queensland Cancer Council (http://www.cancerqld.org.au; A. Mellick), and Griffith Medical Research College, Australia (http://www.qimr.edu.au/research/gmrc/; A. Mellick). A. Swarbrick is a recipient of a Cancer Institute NSW Early Career Development Fellowship grant. The funders had no role in the study design, data collection and analysis, the decision to publish, or the preparation of the manuscript.

The costs of publication of this article were defrayed in part by the payment of page charges. This article must therefore be hereby marked *advertisement* in accordance with 18 U.S.C. Section 1734 solely to indicate this fact.

Received 04/01/2010; revised 06/21/2010; accepted 07/09/2010; published OnlineFirst 08/31/2010.

References

1. Folkman J. Role of angiogenesis in tumor growth and metastasis. Semin Oncol 2002;29:15–8.
2. De Palma M, Venneri MA, Galli R, et al. Tie2 identifies a hematopoietic lineage of proangiogenic monocytes required for tumor vessel formation and a mesenchymal population of pericyte progenitors. Cancer Cell 2005;8:211–26.
3. De Palma M, Mazzieri R, Politi LS, et al. Tumor-targeted interferon-α delivery by Tie2-expressing monocytes inhibits tumor growth and metastasis. Cancer Cell 2008;14:299–311.
4. Yang L, DeBusk LM, Fukuda K, et al. Expansion of myeloid immune suppressor Gr^+CD11b^+ cells in tumor-bearing host directly promotes tumor angiogenesis. Cancer Cell 2004;6:409–21.
5. Marttila-Ichihara F, Auvinen K, Elima K, Jalkanen S, Salmi M. Vascular adhesion protein-1 enhances tumor growth by supporting recruitment of Gr-1^+CD11b^+ myeloid cells into tumors. Cancer Res 2009; 69:7875–83.
6. Lin EY, Nguyen AV, Russell RG, Pollard JW. Colony-stimulating factor 1 promotes progression of mammary tumors to malignancy. J Exp Med 2001;193:727–40.
7. Pollard JW. Tumour-educated macrophages promote tumour progression and metastasis. Nat Rev Cancer 2004;4:71–8.
8. Coussens LM, Werb Z. Inflammation and cancer. Nature 2002;420: 860–7.
9. Nozawa H, Chiu C, Hanahan D. Infiltrating neutrophils mediate the initial angiogenic switch in a mouse model of multistage carcinogenesis. Proc Natl Acad Sci U S A 2006;103:12493–8.
10. Song S, Ewald AJ, Stallcup W, Werb Z, Bergers G. $PDGFR\beta^+$ perivascular progenitor cells in tumours regulate pericyte differentiation and vascular survival. Nat Cell Biol 2005;27:870–9.
11. Kopp HG, Ramos CA, Rafii S. Contribution of endothelial progenitors and proangiogenic hematopoietic cells to vascularization of tumor and ischemic tissue. Curr Opin Hematol 2006;13:175–81.
12. Asahara T, Takahashi T, Masuda H, et al. VEGF contributes to postnatal neovascularization by mobilizing bone marrow derived endothelial progenitor cells. Embo J 1999;18:3964–72.
13. Urbich C, Dimmeler S. Endothelial progenitor cells: characterization and role in vascular biology. Circ Res 2004;95:343–53.
14. Lyden D, Hattori K, Dias S, et al. Impaired recruitment of bone-marrow derived endothelial and hematopoietic precursor cells blocks tumor angiogenesis and growth. Nat Med 2001;7: 1194–201.
15. Ruzinova MB, Schoer RA, Gerald W, et al. Effect of angiogenesis inhibition by Id loss and the contribution of bone-marrow-derived endothelial cells in spontaneous murine tumors. Cancer Cell 2003;4: 277–89.
16. Nolan DJ, Ciarrocchi A, Mellick AS, et al. Bone marrow-derived endothelial progenitor cells are a major determinant of nascent tumor neovascularization. Genes Dev 2007;21:1546–58.
17. Gao D, Nolan DJ, Mellick AS, et al. EPCs control the angiogenic switch in mouse lung metastasis. Science 2008;319:195–8.
18. Bertolini F, Shaked Y, Mancuso P, Kerbel RS. The multifaceted circulating endothelial cell in cancer: towards marker and target identification. Nat Rev Cancer 2006;6:835–45.
19. Shaked Y, Ciarrocchi A, Franco M, et al. Therapy-induced acute recruitment of circulating endothelial progenitor cells to tumors. Science 2006;313:1785–7.
20. Gao D, Mittal V. The role of bone-marrow-derived cells in tumor growth, metastasis initiation and progression. Trends Mol Med 2009;15:333–43.
21. Purhonen S, Palm J, Rossi D, et al. Bone marrow-derived circulating endothelial precursors do not contribute to vascular endothelium and are not needed for tumor growth. Proc Natl Acad Sci U S A 2008; 105:6620–5.
22. Perk J, Gil-Bazo I, Chin Y, et al. Reassessment of Id1 protein expression in human mammary, prostate, and bladder cancers using a monospecific rabbit monoclonal anti-Id1 antibody. Cancer Res 2006;66:10870–7.
23. Lyden D, Young AZ, Zagzag D, et al. Id1 and Id3 are required for neurogenesis, angiogenesis and vascularization of tumour xenografts. Nature 1999;401:670–7.
24. Perry SS, Zhao Y, Nie L, et al. Id1, but not Id3, directs long-term repopulating hematopoietic stem-cell maintenance. Blood 2007;110: 2351–60.
25. Okabe M, Ikawa M, Kominami K, Nakanishi T, Nishimune Y. "Green mice" as a source of ubiquitous green cells. FEBS Lett 1997;407: 313–9.
26. Tudor KS, Deem TL, Cook-Mills JM. Novel α_4-integrin ligands on an endothelial cell line. Biochem Cell Biol 2000;78:99–113.
27. Kumar R, Conklin DS, Mittal V. High-throughput selection of effective RNAi probes for gene silencing. Genome Res 2003;13: 2333–40.
28. Rose'Meyer RB, Mellick AS, Garnham BG, et al. The measurement of adenosine and estrogen receptor expression in rat brains following ovariectomy using quantitative PCR analysis. Brain Res Brain Res Protoc 2003;11:9–18.
29. Campbell RE, Tour O, Palmer AE, et al. A monomeric red fluorescent protein. Proc Natl Acad Sci U S A 2002;99:7877–82.
30. Salmon P, Kindler V, Ducrey O, et al. High-level transgene expression in human hematopoietic progenitors and differentiated blood lineages after transduction with improved lentiviral vectors. Blood 2000;96:3392–8.
31. Perfetto SP, Chattopadhyay PK, Roederer M. Seventeen-colour flow cytometry: unravelling the immune system. Nat Rev Immunol 2004;4: 648–55.
32. Katagiri T, Imada M, Yanai T, et al. Identification of a BMP-responsive element in Id1, the gene for inhibition of myogenesis. Genes Cells 2002;7:949–60.
33. Magalhaes GS, Muotri AR, Marchetto MC, Menck CF, Ventura AM. An adenovirus vector containing the suicide gene thymidine kinase for a broad application in cancer gene therapy. Mem Inst Oswaldo Cruz 2002;97:547–52.
34. Lalor PA, Mapp PI, Hall PA, Revell PA. Proliferative activity of cells in the synovium as demonstrated by a monoclonal antibody, Ki67. Rheumatol Int 1987;7:183–6.
35. Osti D, Marras E, Ceriani I, et al. Comparative analysis of molecular strategies attenuating positional effects in lentiviral vectors carrying multiple genes. Virol Methods 2006;136:93–101.
36. Dickins RA, Hemann MT, Zilfou JT, et al. Probing tumor phenotypes

using stable and regulated synthetic microRNA precursors. Nat Genet 2005;11:1289–95.
37. Peters BA, Diaz LA, Polyak K, et al. Contribution of bone marrow-derived endothelial cells to human tumor vasculature. Nat Med 2005;11:261–2.
38. Duda DG, Cohen KS, Kozin SV, et al. Evidence for incorporation of bone marrow-derived endothelial cells into perfused blood vessels in tumors. Blood 2006;107:2774–6.
39. Yan W, Young AZ, Soares VC, et al. High incidence of T-cell tumors in E2A-null mice and E2A/Id1 double-knockout mice. Mol Cell Biol 1997;12:7317–27.
40. Jankovic V, Ciarrocchi A, Boccuni P, et al. Id1 restrains myeloid commitment, maintaining the self-renewal capacity of hematopoietic stem cells. Proc Natl Acad Sci U S A 2007;104:1260–5.
41. Kaplan RN, Riba RD, Zacharoulis S, et al. VEGFR1-positive haematopoietic bone marrow progenitors initiate the pre-metastatic niche. Nature 2005;438:820–7.
42. Shibuya M. Differential roles of vascular endothelial growth factor receptor-1 and receptor-2 in angiogenesis. J Biochem Mol Biol 2006;39:469–78.
43. Gao D, Nolan D, McDonnell K, et al. Bone marrow-derived endothelial progenitor cells contribute to the angiogenic switch in tumor growth and metastatic progression. Biochim Biophys Acta 2009; 1796:33–40.